

# A predictive model for Covid-19 spread applied to six US states

Zeina S. Khan,  
Frank Van Bussel,  
&

Fazle Hussain\*

Texas Tech University, Department of Mechanical Engineering  
2703 7th Street, Box: 41021, Lubbock, TX 79409

Phone: 806-834-7805

Fax: 806-742-3540

\* fazle.hussain@ttu.edu

September 15, 2022

## Abstract

A compartmental epidemic model is proposed to predict the Covid-19 virus spread. It considers: both detected and undetected infected populations, medical quarantine and social sequestration, plus possible reinfection. The coefficients in the model are evaluated by fitting to empirical data for six US states: California, Louisiana, New Jersey, New York State, Texas, and Washington State. The evolution of Covid-19 is fairly similar among the states: contact and detection rates remain below 5%; however, variations are larger in death rate, recovery rate, and stay-at-home effect. The results reveal that outbreaks may have been well underway in several states before first detected and that some western states might have seen more than one influx of the pandemic. For the majority of states the model's effective reproduction number is slightly above the critical value of one, indicating that Covid-19 will become endemic, spreading for more than two years. Should stay-at-home orders be revoked, most states may experience oscillating yearly infections. Even if additional lockdowns are applied in Texas, and then released according to White House guidelines of 14 days of decreasing cases, a similar endemic situation may occur. Additionally, if lockdowns had been instituted one to three weeks sooner, the number of Covid-19 deaths in New York could have been significantly reduced, but surprisingly not in Texas (perhaps due to aversion to lockdown and absence of a decree).

## Introduction

A cluster of pneumonia cases resulting from an unknown pathogen was identified in December 2019 by Chinese Health authorities in the city of Wuhan (Hubei), China [1]. The pathogen has been identified as a novel strain of coronavirus, SARS-CoV-2 [1], now named Covid-19 [2]. The exponential growth of the disease prompted Chinese authorities to introduce their strictest level of measures to contain its outbreak, including Wuhan city lockdown, banning public gatherings, suspending public transport, and prohibiting travel between cities [3]. Despite these measures, a global pandemic ensued, with 3,855,809 total worldwide cases and 265,861 deaths as of May 9, 2020 as declared by the World Health Organization (WHO) [4].

The first cases of community transmission in the United States were reported in California, Oregon, Washington state and New York state in late February, 2020 [5]. A Santa Clara, California death on Feb. 6 was deemed the country's first Covid-19 fatality after an autopsy was conducted in April [5]. A national emergency was declared by US President Donald Trump on March 13, 2020, and testing several days later revealed that Covid-19 had spread to all 50

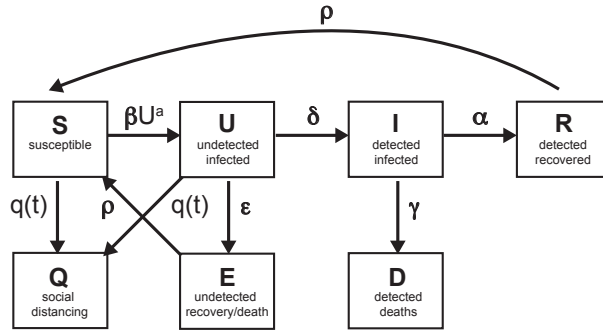


Figure 1: Schematic of the compartments, with the rates of transition between the compartments.

states [5]. On March 20, New York City was declared the US outbreak epicenter [5]. A study, released on April 2020 as a preprint, found via genetic analysis of Covid-19 cases in New York City that the majority of the viruses originated in Europe – revealing that transmissions had begun as early as January from countries with no travel monitoring [6]. As of May 9, 2020, the US had 1,245,874 confirmed Covid-19 cases, and 69,889 Covid-19 deaths [4].

Covid-19 challenges faced by the US include fair allocation of adequate medical resources [7], minimizing mortality, avoiding overwhelming the health-care system, and keeping the effects of lockdown and social distancing policies on the economy within manageable levels [8]. Epidemiological analysis of the virus proliferation and spread is needed to assess the impacts of mitigation strategies including social distancing, sheltering-in-place (voluntary), and quarantines (enforced by authorities) [8]. We have developed a new compartmental model, extending the well-established and celebrated SIR (Susceptible, Infected, Removed) model [9, 10, 11], to evaluate and compare several states’ responses to Covid-19; with this model we can make estimates, using curve fitting of reported empirical data, of the contact rate, the impact of contact-repression measures, the basic reproduction number ( $\mathcal{R}_0$ ), and the dates for the peak numbers of detected and undetected cases. The basic reproduction number of the majority of states examined is found to be larger than the critical value of 1, leading to endemics. We simulated the effect of lifting stay-at-home orders on the dates specified by most of the states examined, and find that the number of infections increases by approximately an order of magnitude, with a yearly oscillation in some states.

## A new model

Our new SQUIDER model incorporates additional processes into the classic SIR (Susceptible, Infected, Recovered) model: i) making a distinction between known cases (which are publicly reported) and asymptomatic or mild cases which are not monitored or detected; ii) including the effects of responses, varying by region, to the pandemic, whether direct, through quarantine or medical isolation of diagnosed cases, or less direct such as social distancing efforts; and iii) possible loss of immunity of recovered individuals, allowing some of them to be reintroduced into the Susceptible population. The model thus requires several new compartments, which we will denote as U (Undetected infected), E (Excluded, meaning undetected recovered and possible deaths), and Q (pseudo-Quarantine, a bin to hold a segment of the susceptible and undetected infected populations, that allows us to model lower contact rates due to social distancing). Furthermore, for modeling/fitting purposes we add a separate compartment D for known infecteds who die; deaths from the virus is a statistic that is generally available [12].

The rate equations are as follows:

$$\frac{dS}{dt} = -\beta S U^a - q(t)S + \rho(E + R) \quad (1)$$

$$\frac{dU}{dt} = \beta SU^a - (q(t) + \epsilon + \delta)U \quad (2)$$

$$\frac{dI}{dt} = \delta U - (\gamma + \alpha)I \quad (3)$$

$$\frac{dR}{dt} = \alpha I - \rho R \quad (4)$$

$$\frac{dD}{dt} = \gamma I \quad (5)$$

$$\frac{dQ}{dt} = q(t)(U + S) \quad (6)$$

$$\frac{dE}{dt} = \epsilon U - \rho E \quad (7)$$

Each compartment is normalized by the total population  $N$  (includes deaths from Covid-19 but not births and deaths from other causes - see below); hence

$$S + Q + U + I + D + E + R = 1. \quad (8)$$

Note that the rates  $\alpha$ ,  $\beta$ ,  $\delta$ ,  $\epsilon$ ,  $\gamma$ , and  $\rho$  are constants (to be evaluated from fits to data).

Before we go through the individual equations we should discuss some of the recurring terms and factors. First, the *incidence rate*  $\beta SU^a$ , the average normalized new infections in time, is nonlinear when  $a > 0$ . Here  $\beta$  is the contact rate, which is the average number of contacts a person has per day, multiplied by the probability of transmitting the disease when contact between a susceptible and an Undetected infected occurs. Detected Infecteds ( $I$ ) are not involved since we assume that, post-diagnosis, the  $I$  group are generally in medical isolation or some other form of quarantine [13]. If  $a = 1$ , this term describes homogenous mixing of the Susceptible and Undetected infected populations [14], which may not be accurate for states with isolated populations, low population densities, or many densely populated areas. Power law incidence rates (such as  $\beta SU^a$ ) have been shown to increase accuracy of SIR models [15, 16].

Second, the factor  $q(t)$  models the effect of social distancing and contact suppression regimes by sequestering a proportion of the Susceptible and Undetected infected populations at a given time  $t^*$ . This does not imply that some large number of undiagnosed people are put into any actual physical quarantine, only that the available compartment sub-groups for infecting ( $U$ ) and becoming infected ( $S$ ) are reduced; alternatively, this could be modeled by altering  $\beta$  or the power law dependency  $a$  in a time-dependent way. Since the ODEs work by transferring populations from one compartment to another over time at different rates, the function  $q(t)$  is implemented as a Gaussian pulse centered at a particular time  $t^*$ , where  $t^*$  is a fit parameter. The standard deviation and height of the pulse are chosen so that a proportion of the population ( $q_{max} = \max(q(t))$ ) is sequestered (this proportion is another fit parameter). This Gaussian form was chosen, as opposed to a constant value used by some authors [17, 18, 19], as many states went into lockdown on a particular day with many people self-isolating [20, 21]. In particular, finding the day  $t^*$  where such a measure starts affecting the number of cases is important, as it reflects the compliance of the state's population. This form for  $q(t)$  allows us to implement the effect of full or partial relaxation of social distancing measures (such as sheltering-at-home); the solver can be given negative pulse strengths, with the sequestered population re-entered into the susceptible population.

Equation 1 for the Susceptible population is reduced nonlinearly by new infections  $\beta SU^a$  due to interactions, and explicitly reduced in a time dependent way by sequestration  $q(t)S$  (not by any significant amount until we get close to the activation time  $t^*$ ), as well as increased again

by re-entrance at a rate  $\rho$  by members of the Excluded ( $E$ ) and Recovered ( $R$ ) groups. This term was added due to the WHO revelation that recovered Covid-19 patients may have little or waning immunity after exposure [22].

Equation 2 for Undetected infecteds, includes the increase due to contact with  $S$  members, and removal by various causes. The rate  $\epsilon$  closely resembles the recovery rate in the basic SIR model, which (since the model is static, implying that births and deaths due to other causes are not considered) implicitly includes deaths due to a potentially fatal disease. Note that, at least in the early days of the pandemic, increased overall deaths in comparison with the prior three years were not examined for signs that the virus was active among undiagnosed populations [23]. The detection rate  $\delta$  specifies the proportion of Undetected infected individuals who are diagnosed with the virus (and are hence no longer undetected); it is added to the  $I$  compartment. Finally, this population is also effectively reduced due to social distancing  $q(t)$ , e.g. residents of many states were encouraged to shelter at home and not seek testing/diagnosis unless they became symptomatic, in order to ease pressure on medical resources [24].

Equation 3 for the detected Infected population, describes increases due to testing at rate  $\delta$  and decreases due to death with rate  $\gamma$ , and recovery with rate  $\alpha$ . Since these individuals are isolated in designated hospital wards or under quarantine at home [13], hence unlikely to be a source of infection to the community at large, we felt there was no need for sequestration (i.e.  $q(t)$ ) when social distancing went into effect. This is in agreement with the WHO guidance on quarantines segregating suspected exposed people [22].

Equation 4 describes the growth of detected Recovered, balanced by outflux of the Recovered population into the susceptible compartment at rate  $\rho$  due to little or waning immunity, expected for human coronaviruses [25]. Equation 5 describes the increase in Deceased detected individuals. Equation 6 describes the increase in the pseudo-Quarantine compartment due to official contact repression measures  $q(t)$ , which as stated above is only significant around the activation time  $t^*$ . Of course, one expects that the coefficients for  $U$  and  $S$  could be different, but are kept the same ( $q(t)$ ) for simplicity, discussed later. Equation 7 describes increases in the undetected recovered population at rate  $\epsilon$ , and decreases in this population due to loss of immunity of  $E$  at rate  $\rho$ . Equation 8 is the trivial statement that the sum of all of these compartments ( $S, Q, U, I, D, E, R$ ) add up to the total population  $N$ .

## Assumptions

Several simplifying assumptions or idealizations have been made. To begin with, in our model the detected Infecteds ( $I$ ) do not transmit the disease to the Susceptible ( $S$ ) population. It is generally the case that in all such disease outbreaks (e.g. the 2014–2016 Ebola outbreak), even when strict quarantine measures are in place, medical service providers and other people rendering direct aid to victims are themselves vulnerable to infection; when the outbreak (in the non-healthcare worker population) is contained they may even make up the substantial proportion of cases [26]. However, in the current situation where the disease circulates through the general population, and safety protocols (such as restricting visitation by friends and relatives) are rigorously enforced by health providers, the number of such cases is statistically negligible.

Other simplifying assumptions: as mentioned above, we have opted to keep our contact rate  $\beta$  constant and instead vary the  $S$  and  $U$  compartment population levels to mimic social distancing effects (for example staying at home). In future versions of our model we may incorporate time dependent  $\beta$  or  $a$  in order to disentangle population wide transmission suppression (e.g. face masks and other protective gear for the public) from social contact suppression (cancellation of concerts and other public gatherings), but for the sake of simplicity in both coding and analysis we have opted for now to use only one time dependent rate. In the same vein, the  $q(t)$  function removes Susceptibles and Undetected infecteds at the same rate (we have no reason at this time to differentiate the rates of change of these populations). Similarly, people

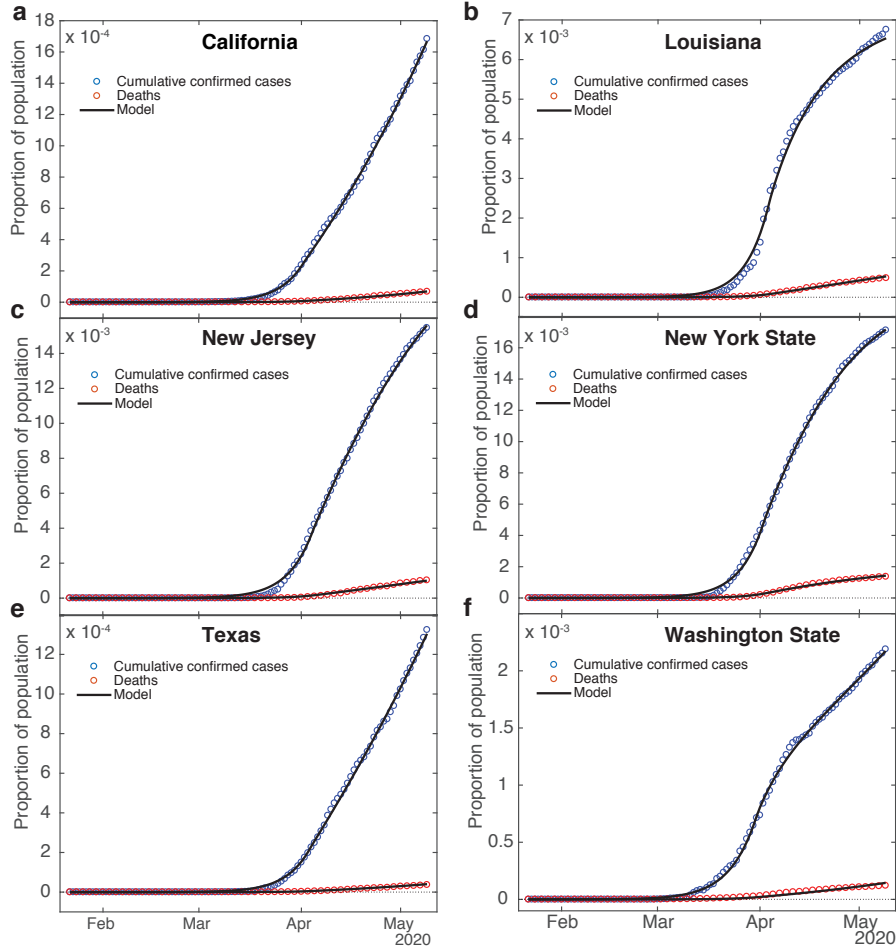


Figure 2: **SQUIDER model fits.** Fits of our compartment model to confirmed cumulative case counts and deaths for (a) California ( $R^2 = 0.9997$ ), (b) Louisiana ( $R^2 = 0.9984$ ), (c) New Jersey ( $R^2 = 0.9994$ ), (d) New York state ( $R^2 = 0.9995$ ), (e) Texas ( $R^2 = 0.9995$ ), and (f) Washington state ( $R^2 = 0.9994$ ). Data was obtained from The Johns Hopkins University [1].

from the Excluded  $E$  and Recovered  $R$  compartments lose immunity at the same rate  $\rho$ . Indeed, it is possible that people who experienced milder forms of the disease ( $E$ ) lose immunity faster than those who experienced more severe symptoms and sought out treatment ( $R$ ); however, we currently do not have any information to justify different rates. Finally, we do not consider the effects of births, vertical transmissions, immigrants, emigrants, or deaths due to other diseases or trauma. The inclusion of deaths due to diagnosed virus cases makes the model not entirely static, but the disease’s total deaths as a proportion of the total population is low enough that births and other such aspects can be safely omitted.

## Results

Figure 2 shows fits of the model to cumulative confirmed case counts and deaths due to Covid-19 for California, Louisiana, New Jersey, New York State, Texas, and Washington State. The fits are all excellent – even for states that have a decreasing trend in case counts. Fit parameters are listed in Table 1. The parameters have similar values across all of the states, where contact and detection rates vary by less than 5%; however, death rate varies by 134%, recovery rate by 82%, and stay-at-home effect by 39%. We compare our fit parameters with the classical SIR model which, to remind the reader, involves only Susceptible, Infected, and Recovered compartments. The  $\beta$  and  $\epsilon$  parameters correspond to the contact and recovery rates of the SIR model; the fit

values imply that for unconstrained epidemic situations (with  $q(t) = \delta = 0$ ) the disease has a reproduction number  $\mathcal{R}_0 = \beta/\epsilon$  of around 5 and a duration of about a week, consistent with prior investigations [19, 28].

It is surprising that the detection rate  $\delta$  is so high ( $\approx 0.5$ ); however, a recent nationwide coronavirus antibody study by the Spanish Health Ministry [29] suggests that the number of unknown infected and unknown recovered in large and heterogeneous jurisdictions, while significant, is not orders of magnitude larger than the number of confirmed cases. This goes against some prior speculation that the asymptomatic and undiagnosed cases might be as much as 10 times the official count [30], which would suggest a detection rate 5 times smaller than our  $\delta$ .

Returning back to figure 2 and table 1, the death rate from diagnosed cases  $\gamma$  falls between around  $1\frac{1}{2}\%$  and  $3\frac{1}{3}\%$ , which is well within the quite wide range of case-fatality rates reported for earlier phases of the pandemic [31]. The recovery rate  $\alpha$  for diagnosed cases, seems somewhat high (in the 0.45 – 0.5 range for New York and New Jersey, and around 0.7 – 0.8 for the other states); this could reflect the fact that detection of any disease would normally occur after that disease has already partly run its course, but it should be kept in mind as well that this compartment has a minimal effect on the size of the fitted compartments  $I$  and  $D$ , so the fitting routine may not be as constrained in selecting the  $\alpha$  value as the other fit parameters. The re-entry rate  $\rho$  is fairly low for most of the states, which indicates that this is not a significant factor for the development of the outbreak within the time period our empirical data covers. Such low  $\rho$  values are not unreasonable since loss of immunity to corona viruses can take months [25]; this is still an open issue for further study. As we see below, this becomes important for longer-term predictions of our model.

Our fitted peak sequestration values range over 0.13 - 0.19; it should be kept in mind this is not the actual quarantining of approximately 15% of the population, but rather the effect of overall reduction in social contacts between susceptible and infectious populations, which in the US was never pursued as systematically or consistently as in some other jurisdictions. The parameter  $t^*$  enables prediction of what day self-isolation policies started having significant effects on case counts. For California this was April 2, Louisiana April 4, New Jersey April 5, New York April 2, Texas April 4, and Washington state March 31. To compare  $t^*$  to states' directives, stay-at-home orders were issued in California on March 19, Louisiana on March 23, New Jersey on March 21, New York on March 22, suggested in Texas on April 2, and issued in Washington on March 23 [32]. The nearly week long time lag between state action and its effect on most of the states should be expected based on the infection lasting about a week as mentioned above. It's possible that Texas residents were following local orders which prescribed sheltering in place sooner than the state orders: Dallas had a state of emergency declared on March 19, and Houston residents were urged to stay at home on March 24 [33].

The initial values of the undetected infecteds  $U(0)$  are all less than one individual (some significantly), implying that none of the states we look at had any actual cases on January 22 (the first day for which we have data). While the ODE results can be scanned to find an estimate for the arrival of the first case (or first two, or five cases) in a jurisdiction, some caution should be exercised in applying this number, since magnitudes at this point are still too small to make statistically valid comparisons. Given that the model estimates there to have been at least 10 cases in all the states studied by the 3rd or 4th week of February (the 1st week of February for New York) we think it is probable that Covid-19 was spreading considerably sooner in New York, New Jersey, Texas, and Louisiana than previously considered, implying that stronger measures – such as travel bans, cluster identification, contact tracing, and quarantine measures – were needed to fully contain the outbreak [34, 35]. California and Washington State had reported cases already in late January, yet both the raw data and our ODE model show the main outbreak occurred well after New York or New Jersey. This is possible if the western states were dealing successfully with cases coming directly from Asia, but lost control of the

parameter	California	Louisiana	New Jersey	New York	Texas	Washington
$\beta$	0.7482	0.7589	0.7614	0.7644	0.7485	0.7511
$a$	0.9943	0.9948	0.9966	0.9970	0.9943	0.9948
$\epsilon$	0.1551	0.1441	0.1390	0.1361	0.1551	0.1545
$\delta$	0.5035	0.5009	0.5073	0.5067	0.5036	0.5055
$\alpha$	0.7324	0.7115	0.5104	0.4426	0.7404	0.8041
$\gamma$	0.0249	0.0213	0.0243	0.0339	0.0191	0.0145
$\rho$	0.0162	0.0750	0.0230	0.0084	0.0144	0.1181
$q_{max}$	0.1382	0.1728	0.1561	0.1894	0.1455	0.1365
$t^*$	72.006	74.200	74.905	72.434	74.127	70.343
$U(0) \times N$	0.0495	0.0265	0.2085	0.6786	0.0208	0.1443

Table 1: SQUIDER model fit parameters for several US states.  $t^*$  values are days counting from January 22, 2020.

outbreak when infected individuals started arriving from the eastern US or possibly Europe; possible differences between the Asian and European strains is are not addressed here.

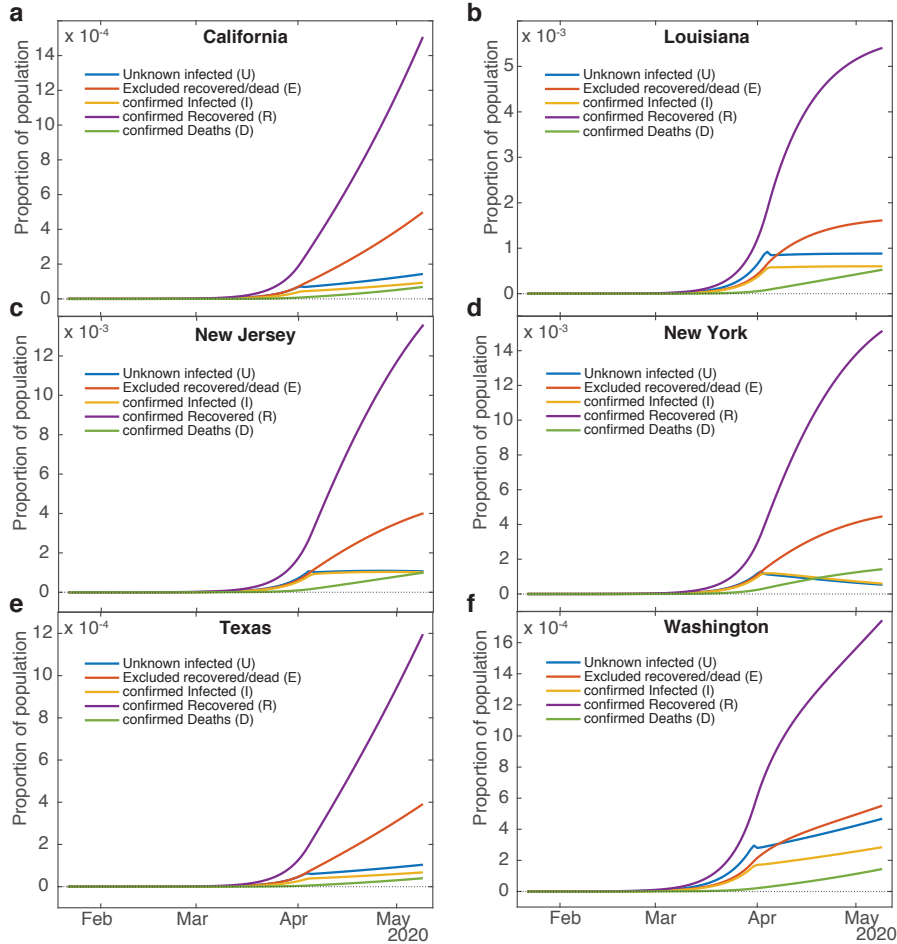


Figure 3: **Computed results for the other compartments for different states.** Unknown infected (U), Excluded due to undetected recovery and deaths (E), confirmed Infected (I), confirmed Recovered (R), and confirmed Deaths (D).

state	$\mathcal{R}_0$
California	1.0498
Louisiana	1.0192
New Jersey	1.0047
New York	0.9648
Texas	1.0439
Washington	1.0257

Table 2: Basic reproduction number  $\mathcal{R}_0$  for the SQUIDER model for several US states.

Figure 3 shows the behaviour of the  $U$ ,  $E$ , and  $R$  compartments, as well as  $I$  and  $D$  (fit populations) over the fit period (January 22 to May 9, 2020). Note that the most striking difference in the shapes of the curves among the states is that between California and Louisiana – the other states lie on the spectrum between them. It appears that sequestering  $S$  and  $U$  populations had a much stronger effect in Louisiana on Recovered and Excluded populations – with plateaus in these populations becoming apparent in April 2020. Similarly, the Unknown infected and confirmed Infected cases rise much less quickly in and beyond April, while the confirmed Deaths continue to rise due to active infections. In contrast, in California, the values for all of the compartments are approximately an order of magnitude smaller, though all of them increase with a steady apparent slope through April and May, suggesting that the outbreak is at an earlier stage. Note that this is possible if California had to deal with a new outbreak of cases as hypothesized above. The effect of applying contact suppression measures (pseudo-quarantine) becomes apparent on day  $t^*$  in  $U$  curves in all of the states as it forms a small hump in the curves (see figure 3). Notably, the states whose undetected infected population  $U$  decreases after quarantine are New Jersey and New York – these states put in strict shelter at home measures [36], whereas, as an example, the Texas governor did not make staying at home mandatory [37] and permitted its residents to attend in-person church services [38].

Table 2 shows the basic reproduction number  $\mathcal{R}_0$  values we have computed for our model among the states selected, using the parameters listed in Table 1 obtained by fitting the model to data and  $\mathcal{R}_0 = \frac{\beta a S_0 U_0^{a-1}}{\delta + \epsilon + q(t)}$ , as defined in the Supplementary Information, equation 11. Note that the epidemic is expected to persist indefinitely if  $\mathcal{R}_0 > 1$ , as is predicted for all states considered except New York. New York’s value is approximately 0.96, likely due to stricter quarantine adherence reflected in the highest  $q_{max}$  value – see Table 1. The other states are predicted to have  $\mathcal{R}_0$  close to, but larger than, unity, suggesting that Covid-19 will not be eradicated unless stricter measures are taken such as increased social distancing and higher quarantine rates. That both extended simulations for dates beyond those for which we have data (shown in figure 4) and  $\mathcal{R}_0$  values predict that New York does not develop an endemic infection gives us some confidence in this prediction. Figure 4 shows that for the majority of the states examined here, if contact suppression is maintained infections will peak and fall at least over the next two years, in the absence of factors such as inter-state migration and vaccination. The peaks for Texas and Washington occur in fall/winter seasons, whereas in California, Louisiana, and New Jersey the peaks occur in the spring/summer seasons. As predicted by the effective reproduction number  $\mathcal{R}_0$ , only New York appears to eradicate the virus by Jan. 2021. The cause of the sharp rise in deaths in New York state in figure 4g is not clear to us; perhaps it is due to early saturation of the health care system [39].

We can generate additional predictions for the effect of lifting shelter-in-place and other social distancing measures, as most of the selected states’ governors have declared re-opening dates – Louisiana on May 15, New Jersey on June 5, New York state on May 15, Texas on April 30, and Washington state on July 12 [32]. Figure 5 shows that the number of infections, both total and detected, increases substantially over the prediction in figure 4, and eventually decay

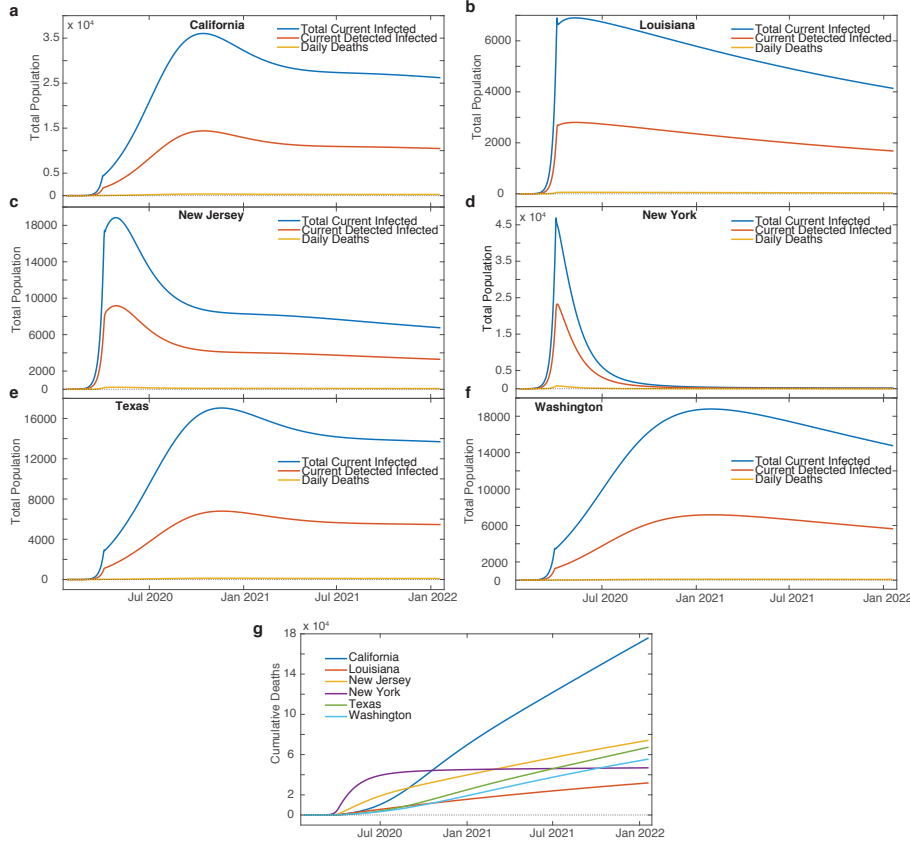


Figure 4: **Model predictions.** Total infected ( $U+I$ ), detected Infected ( $I$ ), and confirmed daily deaths ( $D$ ) for two years beyond the first day of recorded infections for: (a) California, (b) Louisiana, (c) New Jersey, (d) New York, (e) Texas, and (f) Washington state. (g) Cumulative death counts for each state.

for Louisiana and Washington. Should New York and Texas not implement additional measures beyond their re-opening dates – such as contact tracing – a greatly increased peak number of infections, as well as additional smaller peaks (say, due to a secondary wave) may be anticipated. In the absence of any official announcement on the subject by the State of California we test the effect of hypothetical reopening at an arbitrary future date (set conservatively to Sept. 1) and see similar behavior as New York, New Jersey, and Texas. Most of the additional smaller peaks occur in colder months, as is the case for other coronaviruses including the common cold [25] and influenza [40]. All states show oscillatory behavior in the total daily case counts over two years when lockdown measures are lifted, except Louisiana and Washington state. These two states have significantly higher re-entry rates  $\rho$  than the others, and that for oscillations to be present cycling of populations has to occur at an intermediate rate – having a high re-entry rate leads to steady infections; and having no re-entry results in eradication of the virus (see Supplementary Information Sensitivity Analysis and Discussion).

States may reissue stay-at-home orders if the number of cases continues to rise after lifting lockdown; such re-issue is indeed suggested by our model. The possibility of re-imposing the pseudo-quarantine is explored using the fits for Texas, where it is possible that new stay-at-home or lockdown orders would be issued after a large number such as 1,000 new infections per day are detected. Further, a state may choose to reopen after 14 consecutive days of decreasing infections, one of the criteria for state re-opening set by the White House [41]. Figure 6 shows: (a) the increase in confirmed cases after the state is reopened, (b) the rise in cases after a second round of lockdown, and (c) additional increases after a third round of lockdown. From figure 6 we conclude that waiting for 14 days of steady decline in new infections prior to reopening does

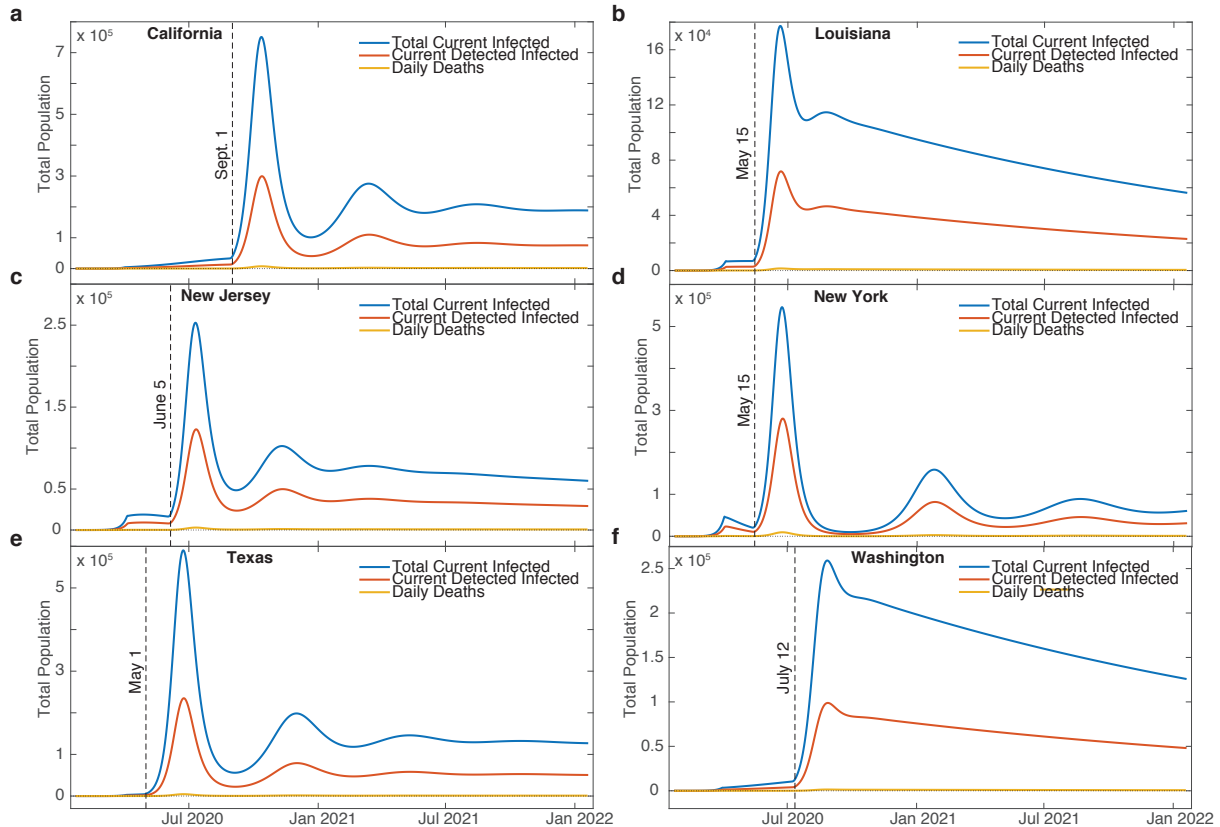


Figure 5: **Predictions for removal of quarantine.** Total infected ( $U+I$ ), detected Infected ( $I$ ), and confirmed daily deaths ( $D$ ) for two years, with the quarantined ( $Q$ ) compartment reintroduced into the susceptible ( $S$ ) compartment on the indicated day set by state policy (except California) for: (a) California, (b) Louisiana, (c) New Jersey, (d) New York, (e) Texas, and (f) Washington state.

not guarantee that a peak in infections is avoided. The number of people sequestered by the second and third lockdowns was set to the  $q_{max}$  determined by fitting to the empirical data. This suggests that multiple pseudo-quarantines can be effective only if more people comply, or spend more time under lockdown.

We tested the effect of increasing the number of consecutive days in pseudo-quarantine for Texas by releasing the pseudo-quarantined after 28 days of decreasing confirmed cases, as suggested by the governors of Delaware and Illinois [42, 43] (figure 7). A similar behavior to reopening after 14 consecutive days of decreasing cases was revealed – the number of cases rise after release – with no significant difference in growth rate and long-term asymptotic behavior – even after two lockdowns. This implies that increased compliance needs to be enforced; contact tracing will inevitably be needed.

Recent counterfactual simulations explored possible Covid-19 outcomes with an alternate history by setting lockdown measures sooner in their metapopulation model (being sets of US county populations connected by individuals who migrate in and out of the sets, such as for work travel) [44]. The virus in the metapopulation was described with a SEIR model (an extended version of the SIR model, which includes an additional compartment for Exposed ( $E$ )), and they predict that New York city would have had 209,987 fewer Covid-19 cases and 17,514 fewer deaths by May 3, 2020, had lockdown measures been implemented one week earlier than March 20 – among other such scenarios of implementing lockdowns sooner by two and three weeks [44]. To see how our novel SQUIDER model compares with this study, we implemented shutdown measures sooner than had been done by setting  $t^*$  to earlier dates for New York State and Texas

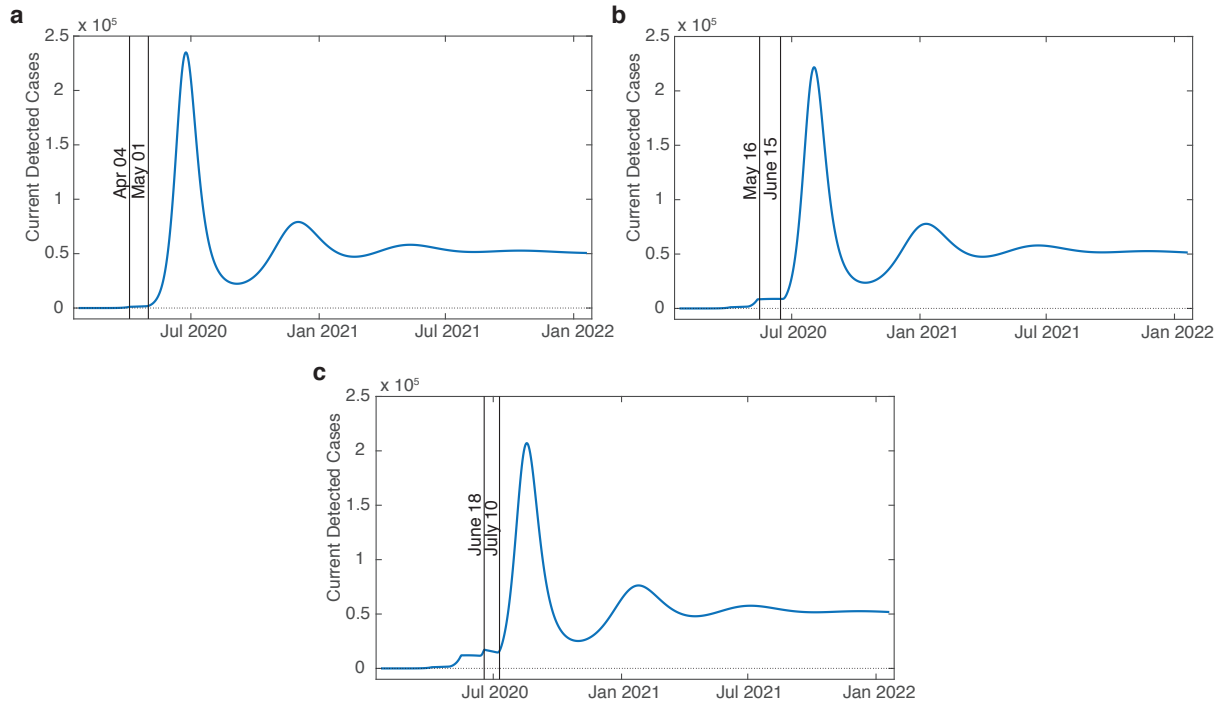


Figure 6: **Predictions for removal of quarantine and its re-application after 14 consecutive days of declining detected cases for Texas.** (a) The predicted number of cases following release of lockdown suggestion following White House policy. Lockdown was applied April 4 and released May 01, 2020. Predicted cases after: (b) a second lockdown applied May 16 (after 1000 new cases are detected) and released June 15, and (c) a third lockdown applied June 18 (after 1000 new cases are detected) and released July 10, 2020.

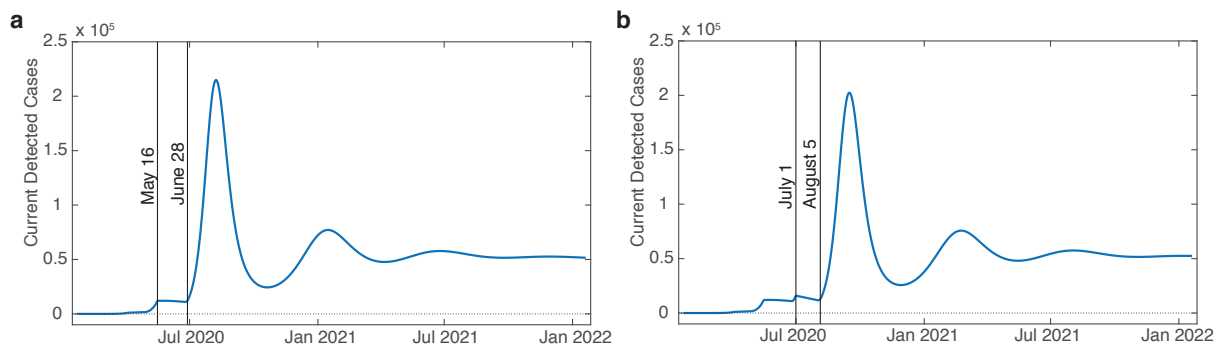


Figure 7: **Predictions for removal of quarantine and its re-application after 28 consecutive days of declining detected cases for Texas.** Predicted cases after: (a) a second lockdown applied on May 16 (after 1000 new cases are detected) and released June 28, and (b) a third lockdown applied on July 1 (after 1000 new cases are detected), and released August 5, 2020.

while  $q_{max}$  was used from our fits, with the lockdown maintained; see figure 8. We similarly find a dramatic decrease in the number of cases and deaths in New York state, whereas Texas shows moderate decreases. For example, our model suggests that had lockdowns occurred one week sooner, by May 3 there would have been  $\approx 12,750$  fewer deaths in New York state and  $\approx 400$  fewer deaths in Texas.

Figure 8a shows that, for all the scenarios, the number of daily infections peaks and declines with the peak decreasing further for each additional week by which lockdown was set back;

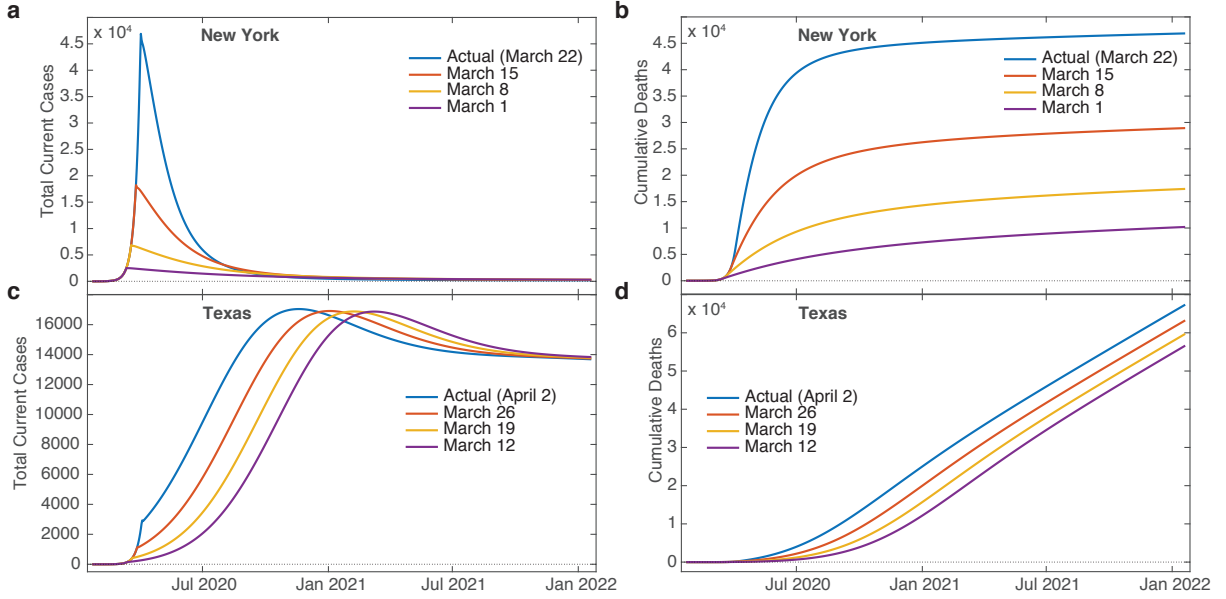


Figure 8: **Effects of applying lockdowns sooner than states had specified.** (a) Predicted total cases ( $U + I$ ), and (b) cumulative deaths for New York state. (c) Predicted total cases, and (d) cumulative deaths for Texas.

similarly in fig. 8b the cumulative deaths plateau to lower levels. In contrast, fig. 8c shows an endemic situation for Texas' daily infections, suggesting the stay-at-home measure one, two, and three weeks sooner pushes the peaks to a later time with slightly smaller values. All curves converge to the same long-term value because the sequestration compliance  $q_{max}$  was not varied from the fit to Texas data. Figure 8d shows that the cumulative deaths in Texas rise steadily regardless of when measures were implemented; however, the number of deaths is reduced for measures implemented earlier. These curves' long-term slopes all increase with the same rate due to keeping the death rate  $\gamma$  at the value from Texas' data fit. Texas' predicted counterfactual model outcomes are likely due to a stable endemic attractor in the model system [45], suggesting that stricter measures (such as increased lockdown compliance and contact tracing) would always have been needed to overcome this outbreak.

## Discussion and Conclusions

Several studies in the peer-reviewed literature and various pre-print servers have modeled the growth of Covid-19 infections and deaths in the US or its various states. One of these uses a SEIR model (Susceptible, Exposed, Infected, Removed) implemented on a network to simulate inter-state travel [46]. They predict that, in the absence of countermeasures, the outbreak peaks on day 54 in their simulation (May 10, 2020). They also predict that on day 50, the number of cases has decreased in New York, New Jersey, Washington, and Louisiana whereas Texas and California have many increasing cases. Other SEIR-type models with additional compartments [17, 18] including quarantine, predict that the US outbreak peaks near May 10, 2020 [17], or peaks in the general population 15 weeks into the outbreak if only 5% of the population practices self-isolation within a day of symptom onset; if 10% of the population self isolates this pushes the peak by an additional 3 weeks, demonstrating that small variations can have significant effects [18].

A Covid-19 SEIRS model (where recovered become susceptible again) including co-infection with additional human coronavirus strains and a periodic basic reproduction number  $\mathcal{R}_0$  corresponding to seasonal forcing, combined with US data, predicts that wintertime outbreaks will occur for several years if immunity wanes – as also occurs with other coronaviruses [47].

This study also predicts that the number of confirmed Covid-19 cases in the first wave strongly depends on the peak value of  $\mathcal{R}_0$ . Furthermore, social distancing was tested by reducing  $\mathcal{R}_0$ ; applied once this may push the epidemic peak to the autumn, whereas intermittent application can reduce the total number of cases [47].

As expected for nonlinear systems, some predictions, even if accurate for a short time, can deviate significantly with increased time. A logistic model of Covid-19 growth in the US predicts that the cumulative number of cases plateaus by May 14, 2020 [48]. Alternatively, a neural network parametric model was developed, which predicted that the US would reach the peak number of cases by April 8, 2020 [49]. Additionally, a sigmoidal Hill-type model predicts that the US will have 735,920 cases within 76 days of the outbreak, with 41,285 deaths [50]. In contrast, our model predicts significantly more Covid-19 cases and deaths, with an extended duration past 2 years for the majority of states examined. Note: all disease models come with drawbacks. Our model is not mechanistic; it says nothing about Covid-19 specifically. While the quality of our fits to current data is very good, the accuracy of the projections depends on the reliability of the data used to generate the fit parameters.

Delays in transitions between compartments (such as our pseudo-quarantine), and in transitioning between several compartments (effectively causing a delay) prior to re-entry in the susceptible population are known to cause oscillations in SIR type models [45] – reintroducing individuals into the susceptible compartment de-stabilizes the steady rate of infections. Temporary immunity, modeled by our reintroduction of recovered and excluded populations into the susceptible compartment, produces yearly oscillations such as found in influenza and other human corona viruses (i.e. “common colds”) [51, 25]. It is quite likely that Covid-19 will become endemic in the United States with yearly spikes in cases.

We have chosen to not include vaccination in our model, even though the race for development is currently underway [52]; rather we have focussed on non-medical interventions. Including such an effect is feasible in our model, where vaccinations would reduce the susceptible population. This could be at a constant rate, such as for newborn infants receiving the measles-mumps-rubella vaccine [53], or it could be a time dependent term reflecting people’s confidence in vaccinations [54]. We look forward to seeing the effect of vaccination on our model predictions once Covid-19 vaccination has been demonstrated to be safe and effective in both animals and humans – estimated to be possible by autumn 2021 [55].

In conclusion, we have developed a compartment model taking into account social distancing, undetected infecteds, and possible loss of immunity – all issues which are relevant for Covid-19. The model describes current data very well for the states selected for study; this more realistic picture of the disease growth is likely due to both using a larger number of compartments than traditional SIR-type models, and to considering additional nonlinearity in the infectious power of the disease. While projections based on the model are not wholly optimistic, they do point to the fact that it is quite possible to avoid more severe outcomes with stronger measures than have been pursued so far.

## Methods

Please refer to the Supplementary Information: Methods.

## Competing Interests

The authors declare no competing interests

## Acknowledgements

This study was supported by TTU President’s Distinguished Chair Funds. We acknowledge early encouragement by Dr. Jamilur R. Choudhury to study Covid-19, and humbly dedicate this paper to his memory.

## References

- [1] World Health Organization. Novel coronavirus – China. Technical report, World Health Organization, 2020.
- [2] World Health Organization et al. Coronavirus disease 2019 (COVID-19): situation report, 22. Technical report, World Health Organization, 2020.
- [3] Huaiyu Tian, Yonghong Liu, Yidan Li, Moritz UG Kraemer, Bin Chen, Chieh-Hsi Wu, Jun Cai, Bingying Li, Bo Xu, Qiqi Yang, et al. Early evaluation of transmission control measures in response to the 2019 novel coronavirus outbreak in China. *medRxiv*, 2020.
- [4] World Health Organization et al. Coronavirus disease 2019 (COVID-19): situation report, 110. Technical report, World Health Organization, 2020.
- [5] Erin Schumaker. Timeline: How coronavirus got started. *ABC news*, 2020.
- [6] Ana S Gonzalez-Reiche, Matthew M Hernandez, Mitchell Sullivan, Brianne Ciferri, Hala Alshammary, Ajay Obla, Shelcie Fabre, Giulio Kleiner, Jose Polanco, Zenab Khan, et al. Introductions and early spread of SARS-CoV-2 in the New York City area. *medRxiv*, 2020.
- [7] Ezekiel J Emanuel, Govind Persad, Ross Upshur, Beatriz Thome, Michael Parker, Aaron Glickman, Cathy Zhang, Connor Boyle, Maxwell Smith, and James P Phillips. Fair allocation of scarce medical resources in the time of Covid-19, 2020.
- [8] Roy M Anderson, Hans Heesterbeek, Don Klinkenberg, and T Déirdre Hollingsworth. How will country-based mitigation measures influence the course of the COVID-19 epidemic? *The Lancet*, 395(10228):931–934, 2020.
- [9] Fred Brauer, Carlos Castillo-Chavez, and Zhilan Feng. Simple compartmental models for disease transmission. In *Mathematical Models in Epidemiology*, pages 21–61. Springer, 2019.
- [10] Michael Small, Pengliang Shi, and Chi Kong Tse. Plausible models for propagation of the SARS virus. *IEICE transactions on fundamentals of electronics, communications and computer sciences*, 87(9):2379–2386, 2004.
- [11] Hyuk-Jun Chang. Estimation of basic reproduction number of the Middle East respiratory syndrome coronavirus (MERS-CoV) during the outbreak in South Korea, 2015. *Biomedical Engineering Online*, 16(1):79, 2017.
- [12] Coronavirus COVID. Global cases by the Center for Systems Science and Engineering (CSSE) at Johns Hopkins University. *Coronavirus Resource Center*. April, 17:2020, 19.
- [13] Wendy E Parmet and Michael S Sinha. Covid-19? the law and limits of quarantine. *New England Journal of Medicine*, 382(15):e28, 2020.
- [14] Xinzhi Liu and Peter Stechliniski. Infectious disease models with time-varying parameters and general nonlinear incidence rate. *Applied Mathematical Modelling*, 36(5):1974–1994, 2012.

- [15] Artem S Novozhilov. Epidemiological models with parametric heterogeneity: Deterministic theory for closed populations. *Mathematical Modelling of Natural Phenomena*, 7(3):147–167, 2012.
- [16] Manojit Roy and Mercedes Pascual. On representing network heterogeneities in the incidence rate of simple epidemic models. *ecological complexity*, 3(1):80–90, 2006.
- [17] Conghui Xu, Yongguang Yu, QuanChen Yang, and Zhenzhen Lu. Forecast analysis of the epidemics trend of COVID-19 in the United States by a generalized fractional-order SEIR model. *arXiv preprint arXiv:2004.12541*, 2020.
- [18] Seyed M Moghadas, Affan Shoukat, Meagan C Fitzpatrick, Chad R Wells, Pratha Sah, Abhishek Pandey, Jeffrey D Sachs, Zheng Wang, Lauren A Meyers, Burton H Singer, et al. Projecting hospital utilization during the COVID-19 outbreaks in the United States. *Proceedings of the National Academy of Sciences*, 117(16):9122–9126, 2020.
- [19] Benjamin F Maier and Dirk Brockmann. Effective containment explains subexponential growth in recent confirmed COVID-19 cases in China. *Science*, 2020.
- [20] Lawrence O Gostin, James G Hodge, and Lindsay F Wiley. Presidential powers and response to COVID-19. *Jama*, 2020.
- [21] Sarah Mervosh, Denise Lu, and Vanessa Swales. See which states and cities have told residents to stay at home. *New York Times*, 2020.
- [22] World Health Organization et al. “Immunity passports” in the context of COVID-19: scientific brief, 24 April 2020. Technical report, World Health Organization, 2020.
- [23] Daniel Weinberger, Ted Cohen, Forrest Crawford, Farzad Mostashari, Don Olson, Virginia E Pitzer, Nicholas G Reich, Marcus Russi, Lone Simonsen, Annie Watkins, et al. Estimating the early death toll of COVID-19 in the United States. *Medrxiv*, 2020.
- [24] Centers for Disease Control and Prevention. Evaluating and testing persons for coronavirus disease 2019 (COVID-19). *National Center for Immunization and Respiratory Diseases (NCIRD), Division of Viral Diseases*, 2020.
- [25] KA Callow, HF Parry, M Sergeant, and DAJ Tyrrell. The time course of the immune response to experimental coronavirus infection of man. *Epidemiology & Infection*, 105(2): 435–446, 1990.
- [26] Centers for Disease Control and Prevention. 2014-2016 Ebola outbreak in West Africa. <https://www.cdc.gov/vhf/ebola/history/2014-2016-outbreak/index.htm>, Last reviewed March 8, 2019. Majority of cases in U.S. were healthcare workers; see section “Ebola in the United States”.
- [1] Johns Hopkins University. [https://github.com/CSSEGISandData/COVID-19/tree/master/csse\\_covid\\_19\\_data/csse\\_covid\\_19\\_time\\_series](https://github.com/CSSEGISandData/COVID-19/tree/master/csse_covid_19_data/csse_covid_19_time_series), 2020.
- [28] Ying Liu, Albert A Gayle, Annelies Wilder-Smith, and Joacim Rocklöv. The reproductive number of COVID-19 is higher compared to SARS coronavirus. *Journal of travel medicine*, 2020.
- [29] Jessica Jones. Spanish antibody study points to 5% of population affected by coronavirus. *Reuters*, May 2020. URL <https://www.reuters.com/article/us-health-coronavirus-spain-study/spanish-antibody-study-points-to-5-of-population-affected-by-coronavirus-idUSKBN22P2RP>. Study was conducted by the Carlos III Institute for Health and the Spanish National Statistics Institute.

- [30] Giuseppe Gaeta. A simple SIR model with a large set of asymptomatic infectives. *arXiv preprint arXiv:2003.08720v1*, 2020.
- [31] Max Roser, Hannah Ritchie, Esteban Ortiz-Ospina, and Joe Hasell. Mortality risk of COVID-19. *Our World in Data*, 2020. <https://ourworldindata.org/mortality-risk-covid>.
- [32] Sarah Mervosh, Jasmine C. Lee, and Nadja Popovich. See which states are reopening and which are still shut down. *The New York Times*, 2020.
- [33] Paul Debenedetto and Katie Watkins. Harris County orders public to stay indoors amid coronavirus pandemic. *Houston Public Media*, 2020.
- [34] Francesco Pinotti, Laura Di Domenico, Ernesto Ortega, Marco Mancastroppa, Giulia Pulano, Eugenio Valdano, Pierre-Yves Boelle, Chiara Poletto, and Vittoria Colizza. Lessons learnt from 288 COVID-19 international cases: importations over time, effect of interventions, underdetection of imported cases. *medRxiv*, 2020.
- [35] Matteo Chinazzi, Jessica T Davis, Marco Ajelli, Corrado Gioannini, Maria Litvinova, Stefano Merler, Ana Pastore y Piontti, Kunpeng Mu, Luca Rossi, Kaiyuan Sun, et al. The effect of travel restrictions on the spread of the 2019 novel coronavirus (COVID-19) outbreak. *Science*, 368(6489):395–400, 2020.
- [36] Isabel Togoh and Lisette Voytko. Bay area will reportedly order residents to ‘shelter in place’ as states ramp up coronavirus lockdown measures. *Forbes*, 2020.
- [37] Patrick Svitek. Gov. Greg Abbott isn’t calling it a stay-at-home order. But he’s telling Texans to stay at home. *The Texas Tribune*, 2020.
- [38] Devon Link. Fact check: Yes, Texas’ governor has deemed religious services essential amid pandemic. *USA Today*, 2020.
- [39] Lizzie Widdicombe. The Coronavirus Pandemic Peaks in New York’s Hospitals. *The New Yorker*, 2020.
- [40] Terho Heikkinen and Asko Järvinen. The common cold. *The Lancet*, 361(9351):51–59, 2003.
- [41] White House. Guidelines: opening up America again, 2020.
- [42] Lauren Lantry. What’s your state’s coronavirus reopening plan? *abc NEWS*, 2020.
- [43] Mary Hansen. The regions and phases of Pritzker’s plan to reopen Illinois. *NPR Illinois*, 2020.
- [44] Sen Pei, Sasikiran Kandula, and Jeffrey Shaman. Differential effects of intervention timing on COVID-19 spread in the united states. *medRxiv*, 2020.
- [45] Herbert W Hethcote, Harlan W Stech, and Pauline Van Den Driessche. Nonlinear oscillations in epidemic models. *SIAM Journal on Applied Mathematics*, 40(1):1–9, 1981.
- [46] Mathias Peirlinck, Kevin Linka, Francisco Sahli Costabal, and Ellen Kuhl. Outbreak dynamics of COVID-19 in China and the United States. *Biomechanics and Modeling in Mechanobiology*, page 1, 2020.
- [47] Stephen M Kissler, Christine Tedijanto, Edward Goldstein, Yonatan H Grad, and Marc Lipsitch. Projecting the transmission dynamics of SARS-CoV-2 through the postpandemic period. *Science*, 2020.

- [48] Levente Kriston and Levente Kriston. Projection of cumulative coronavirus disease 2019 (COVID-19) case growth with a hierarchical logistic model. *Bull World Health Organ COVID-19 Open Preprints*. <http://dx.doi.org/10.2471/BLT>, 20, 2020.
- [49] Steffen Uhlig, Kapil Nichani, Carsten Uhlig, and Kirsten Simon. Modeling projections for COVID-19 pandemic by combining epidemiological, statistical, and neural network approaches. *medRxiv*, 2020.
- [50] Yasser Aboelkassem. COVID-19 pandemic: A Hill type mathematical model predicts the US death number and the reopening date. *medRxiv*, 2020.
- [51] Yuliya N Kyrychko and Konstantin B Blyuss. Global properties of a delayed SIR model with temporary immunity and nonlinear incidence rate. *Nonlinear analysis: real world applications*, 6(3):495–507, 2005.
- [52] T Thanh Le, Zacharias Andreadakis, Arun Kumar, R Gomez Roman, Stig Tollefsen, Melanie Saville, and Stephen Mayhew. The COVID-19 vaccine development landscape. *Nature Reviews Drug Discovery*, 19:305–6, 2020.
- [53] Boris Shulgin, Lewi Stone, and Zvia Agur. Pulse vaccination strategy in the SIR epidemic model. *Bulletin of mathematical biology*, 60(6):1123–1148, 1998.
- [54] Alberto d’Onofrio and Piero Manfredi. Bifurcation thresholds in an SIR model with information-dependent vaccination. *Mathematical Modelling of Natural Phenomena*, 2(1): 26–43, 2007.
- [55] Lynne Peeples. News feature: Avoiding pitfalls in the pursuit of a COVID-19 vaccine. *Proceedings of the National Academy of Sciences*, 117(15):8218–8221, 2020.
- [2] United States Census Bureau. <https://www2.census.gov/programs-surveys/popest/datasets/2010-2019/national/totals>, 2020.
- [3] *Optimization Toolbox User’s Guide: Least-Squares (Model Fitting) Algorithms*. The MathWorks, Inc., r2017a edition, March 2017.
- [4] Pauline van den Driessche. Reproduction numbers of infectious disease models. *Infectious Disease Modelling*, 2(3):288–303, 2017.

# A predictive model for Covid-19 spread applied to six US states: Supplementary Information

## Methods

All numerical simulation for equations 1-8, fits, and data management were done in MATLAB. Data for cumulative confirmed cases and deaths were obtained from the Johns Hopkins University (JHU) Center for Systems Science and Engineering, which has been making highly credible US and global Covid-19 time-series statistics available to the public on the GitHub [1] website. Raw data in the original CSV files were converted to Matlab `table` data structures for ease of access; since the US data were broken out by municipality/county, it was necessary to aggregate this to create each state wide time series. 2019 estimates of state populations used for normalization were acquired from the US Census Bureau [2].

Fits (least squares) of numerically generated curves to the data were obtained using Matlab's `lsqcurvefit` using a *trust-region-reflective* algorithm [3]. One of the benefits of this fitting routine is that fit parameters can be given bounds or fixed values (the latter being especially useful during model development and testing). Fit parameters were: all model rate parameters ( $\beta$ ,  $\epsilon$ ,  $\delta$ ,  $\alpha$ ,  $\gamma$ , and  $\rho$ ), power law exponent  $a$ , initial condition for unknown infecteds  $U(0)$ , plus two parameters governing sequestration of populations due to social distancing – peak  $q$  value and date of application  $t^*$ . Since all the rates are bound between 0 and 1, the  $t^*$  parameter was rescaled by the total time of the simulation to fall within the same range (this helps the fitting routine when determining step sizes while revising the current solution). Fits were made comparing certain selected and/or aggregated simulation results against normalized JHU data for cumulative confirmed cases and deaths, simultaneously. `lsqcurvefit` default values were used for tolerances, iterations, and step size, but because the proportions of state populations were so small simulation results and normalized data were rescaled to increase the magnitude of the error, preventing the fit routine from prematurely settling for a solution (the scaling formula was chosen so that the norm of the rescaled test data was equal to the number of elements in the test data matrix).

Simulation results were generated using Matlab's `ode45` function, which uses an explicit Runge-Kutta (4, 5) formula. Default settings were used for the solver, except that the maximum step-size was constrained to be  $\leq 0.5$  days (this prevents the solver, which uses an adaptive step-size, from accidentally stepping over the sequestration date  $t^*$ ). The implementation of the model itself, coded in a function that is given as an argument to `ode45`, is for the most part straightforward; the only aspect that requires any further comment is the handling of the sequestration function  $q(t)$ .

As mentioned above, sequestration is modelled as a smoothly shaped pulse centered at time  $t^*$ . Since the system of ODEs works by transferring populations at various rates between compartments, in practice we set a temporary rate which changes every time the solver calls the model subroutine. For this we use the value of a Gaussian curve at  $x = t$  with mean value  $t^*$ , height normalized, and width set so as to achieve the sequestration we desire (easily calculated using Matlab's `normpdf` function). Since `ode45`'s adaptive step-size decreases when it detects unexpected movement in the  $q$  rate, a well resolved sampling of different values near the peak  $t^*$  is obtained. To make analysis more straightforward, we decided that the peak rate given to the solver would be equal to the total sequestration effect (e.g., if we set the peak rate to 0.15, then roughly 15% of the  $S$  and  $U$  compartments would ultimately be moved into the  $Q$  compartment). To achieve this, for peak rates  $\leq 0.625$  we normalized the height to the peak rate, and set the standard deviation to a value between 0.4 and 0.625 determined by trial and error and fit to a cubic polynomial. For peak rates above 0.625, a much more complicated formula was needed to achieve the desired effect; since such high sequestration never appeared in any of the fits we will omit any further discussion of this, except to say that to get effective clearance (99.84%) of the entire relevant compartments we use a Gaussian with both height and

width set to  $\approx 1.6$ .

Lastly, for the purpose of doing projections the model implementation subroutine accepts an arbitrary number of peak rate/activation date pairs tacked onto the end of the parameter vector it takes as one of its arguments. This allows us to test the effect of doing several interventions of possibly different magnitudes. Also, a negative peak rate is implemented as returning the specified proportion of the sequestered population in  $Q$  back to  $S$  (since `ode45` has no facility for keeping track of the ratio of  $S$  and  $U$  populations that were originally sequestered, it was felt that returning everyone to  $S$  was the most sensible approach). To make this feasible codewise, at any particular time  $t$  only the  $q_i$  with peak time  $t_i^*$  closest to  $t$  is executed. In practice, if peaks are set too close to each other (e.g. within half a week or so) they may interfere with each other's ability to achieve full sequestration or release; but since this is essentially the case in real life as well we thought it not to be a priority to address this issue.

## The reproduction number $\mathcal{R}_0$

In epidemiology,  $\mathcal{R}_0$  is “the basic reproduction number of a disease” and denotes the expected number of cases produced by a single infected individual in a completely susceptible population. This number, extensively used in epidemiological modeling, describes whether an epidemic breaks out or not; if the value is less than 1 an outbreak does not result in an epidemic, whereas if it is larger than 1 an epidemic occurs [4]. Hence if it close to 1, this has implications. For a value slightly smaller than 1, the outbreak will eventually go away, and for a value slightly larger than one the outbreak does not. If  $\mathcal{R}_0$  is much larger than 1, then the outbreak will be stronger and faster. In simple SIR models, it is the product of transmissibility (a probability or likelihood of becoming infected), contact rate (the amount of time needed in contact in order to be infected), and duration of infectiousness (time to recover), namely  $\beta/\alpha$ . Our model is more complex (due to the seven identified compartments); therefore  $\mathcal{R}_0$  must involve additional factors such as  $q(t)$ ,  $\rho$ ,  $\epsilon$ ,  $\delta$ , as well as initial conditions. To compute  $\mathcal{R}_0$ , we follow the method outlined by van den Driessche [4].

Let  $x = (x_1, x_2, \dots, x_n)$  be the number of individuals in each compartment, where  $m < n$  compartments contain infected individuals – here the  $U$  and  $I$  compartments. Consider the model equations written in the form  $\frac{dx_i}{dt} = \mathcal{F}_i(x) - \mathcal{V}_i(x)$  for  $i = 1, 2, \dots, m$ . Here  $\mathcal{F}_i(x)$  is the rate of appearance of new infections in compartment  $i$  (i.e. positive terms), and  $\mathcal{V}_i(x)$  is the rate of transitions between compartment  $i$  and other infected compartments (i.e. negative terms). It is assumed that  $\mathcal{F}_i = 0$  if  $i \in [m + 1, n]$ ; i.e. it is zero for compartments that do not describe infected populations. Define matrices  $F = \left[ \frac{\partial \mathcal{F}_i(x(0))}{\partial x_j} \right]$  and  $V = \left[ \frac{\partial \mathcal{V}_i(x(0))}{\partial x_j} \right]$  for  $1 \leq i, j \leq m$ . Let  $\psi(0)$  be the number of infected and undetected infected at the initial time of detection. Then  $FV^{-1}\psi(0)$  gives the expected number of new infections; i.e. the matrix  $FV^{-1}$  has the  $(i, j)$  item equal to the expected number of secondary infections in compartment  $i$  produced by an infected individual introduced in compartment  $j$ . Then  $\mathcal{R}_0$  is given by the largest positive eigenvalue of  $FV^{-1}$ .

For our model,

$$F = \begin{bmatrix} \beta a S_0 U_0^{a-1} & 0 \\ \delta & 0 \end{bmatrix}, \quad (9)$$

$$V = \begin{bmatrix} \epsilon + \delta + q(t) & 0 \\ 0 & \alpha + \gamma \end{bmatrix}, \quad (10)$$

which yields

$$\mathcal{R}_0 = \frac{\beta a S_0 U_0^{a-1}}{\delta + \epsilon + q(t)}, \quad (11)$$

where  $S_0 = S(0) \approx 1$  and  $U_0 = U(0)$  is a fit parameter. Note that  $F$  and  $V$  are  $2 \times 2$  matrices because we have only two compartments of infected populations – Infected ( $I$ ) and Undetected

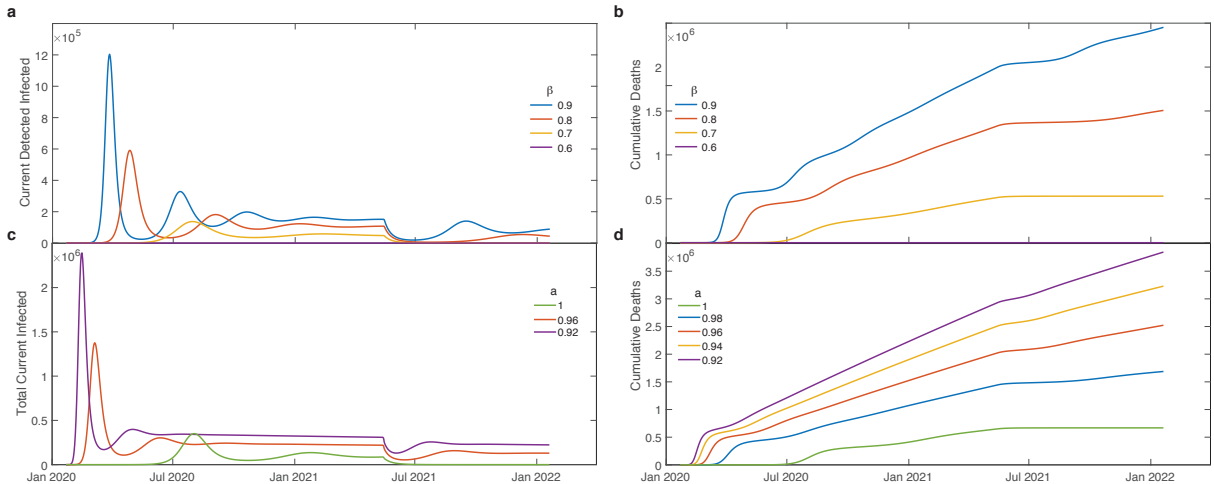
infected ( $U$ ). Considering that  $q$  is time dependent, we use its maximum value to estimate  $\mathcal{R}_0$ ; so  $q_{max}$  represents the best scenario for fastest eradication of the virus.

## Sensitivity analysis

We vary the values of the parameters from the California fits to determine the model sensitivity to those values. Starting with the parameters in the nonlinear term  $\beta SU^a$  in equation 2,

$$\frac{dU}{dt} = \beta SU^a - q(t)U - \epsilon U - \delta U,$$

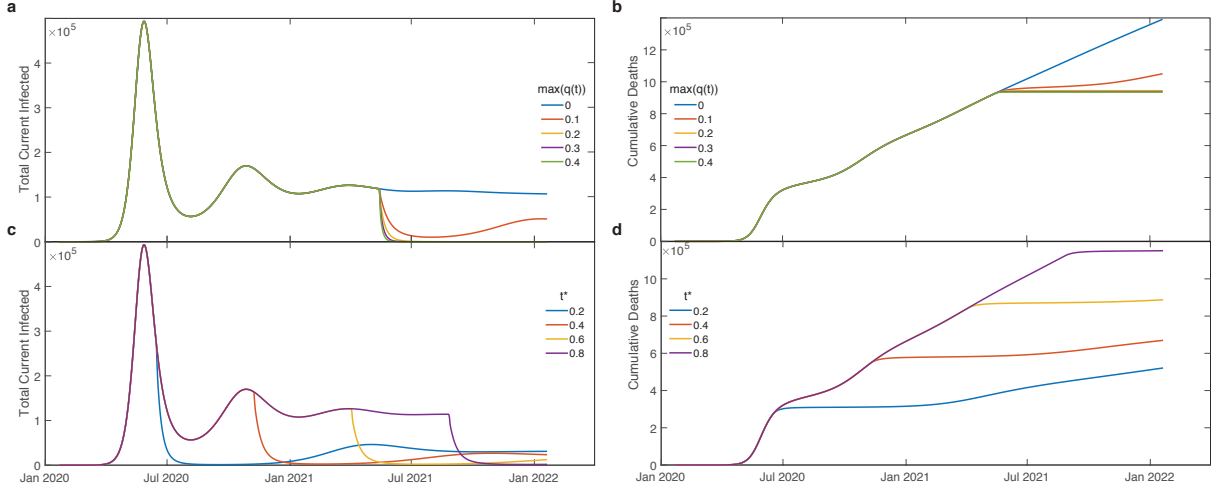
$\beta$  and  $a$  (see supplementary figure 1), note that the model is very sensitive to small changes in  $\beta$ , and particularly  $a$ , which is to be expected for these driving parameters of the infection. In particular, increasing  $\beta$  decreases the time to achieve a peak in the daily case count and increases the peak value – expected if the disease were more contagious, contacts were increased between the  $S$  and  $U$  populations, or both. Increasing  $\beta$  also raises the number of cumulative deaths faster. Decreasing  $a$  has a similar effect (since all compartments are rescaled to have a value less than one); as  $a$  is decreased by very small increments, the peak number of deaths increases and occurs sooner in time, and the cumulative deaths increase faster. Lowering  $a$  increases the infectious power of the virus.



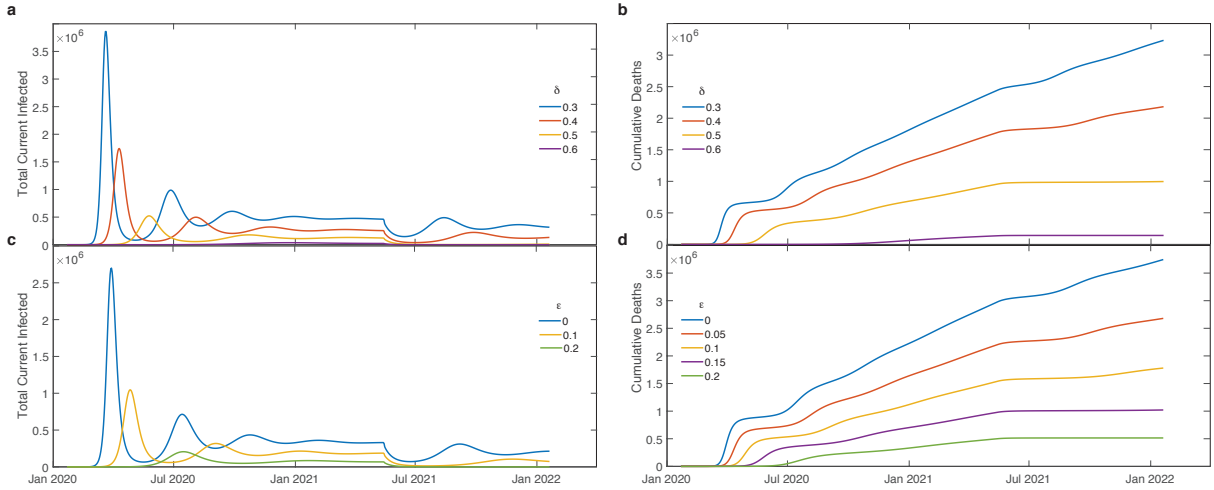
Supplementary Figure 1: **Effect of varying contact rate  $\beta$  and infective power  $a$  on the total infected population and deaths.** (a) Total infected, and (b) deaths for  $\beta$  values ranging from 0.6-0.9. (c) Total infected, and (d) deaths for  $a$  values ranging from 0.98-1. California fits were used for this comparison.

In supplementary figure 2, the effect of varying the peak pseudo-quarantine value  $q_{max}$ , and time of application  $t^*$  are shown. The value of  $q_{max}$  has little effect on timing for the peaks in the total infected population; rather it affects the late time behavior of both total infected and deceased populations. The number of daily infections drops off after about a year past the peak date as the number of susceptible individuals available to infect decreases as  $q_{max}$  increases; the cumulative number of deaths drop off at a similar time as well. We also observe that moving  $t^*$  back in time reduces secondary infection peaks and deaths. As  $t^*$  is increased, the number of daily infections and cumulative deaths drop off at a later time; this is expected as a fraction of the population is removed from the susceptible compartment at a later time.

supplementary figure 3(a)-(b) shows that increasing detection rate  $\delta$  reduces the total number of infections and cumulative deaths; this is to be expected as detection reduces the number of infecteds affecting the susceptible population. A similar effect is observed for increasing the exclusion rate  $\epsilon$  due to undetected recovery shown in supplementary figure 3(c)-(d).



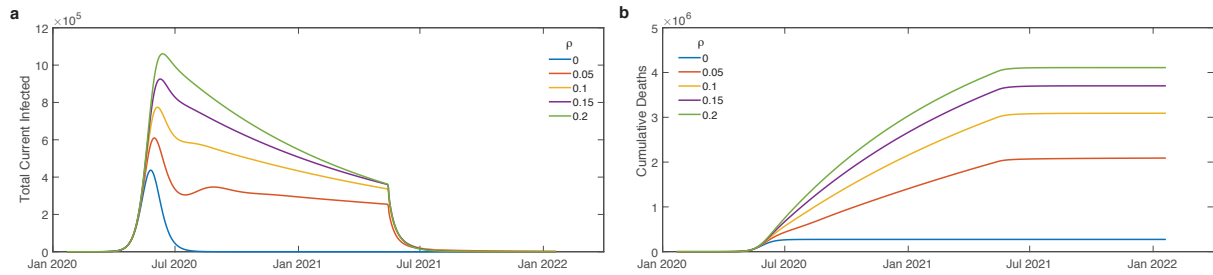
Supplementary Figure 2: **Effect of varying peak pseudo-quarantine rate  $q_{max}$  and time applied  $t^*$  on the total infected population and deaths.** (a) Total infected, and (b) deaths for  $q_{max}$  values ranging from 0-0.4. (c) Total infected, and (d) deaths for  $t^*$  values ranging from 0.2-0.8. California fits were used for this comparison.



Supplementary Figure 3: **Effect of varying exclusion rate  $\epsilon$  and detection rate  $\delta$  on the total infected population and deaths.** (a) Total infected, and (b) deaths for  $\delta$  values ranging from 0.3-0.6. (c) Total infected, and (d) deaths for  $\epsilon$  values ranging from 0-0.2. California fits were used for this comparison.

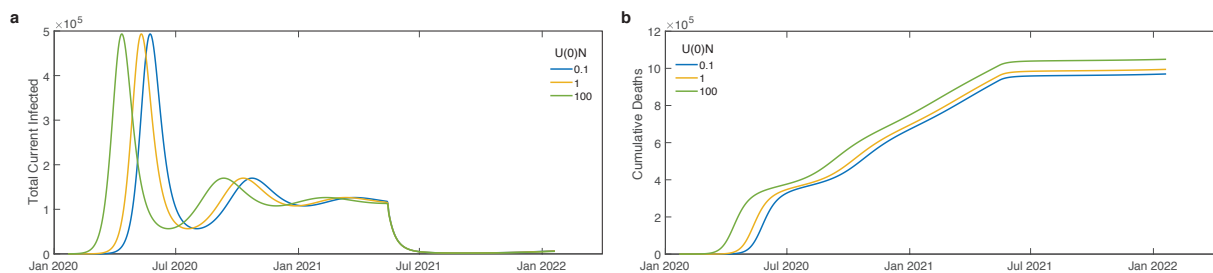
We determine that increasing the re-entry rate  $\rho$  broadens the late-time tail of the daily total infection curve and increases the number of deaths, shown in supplementary figure 4(a)-(b). This occurs due to increasing the number of susceptible individuals available to infect at a steady rate. Also note that, for certain  $\rho$  values, a secondary peak emerges, whereas as  $\rho$  is further increased, the secondary peak disappears. This is due to an instability in the number of infections as  $\rho$  increases; when it is large enough the number of new infections stabilizes.

We also find that increasing the number of initially undetected infected people  $U(0)$  shifts the peak of the current total infected population earlier in time but does not significantly alter the peak value, and slightly increases the number of deaths, shown in supplementary figure 5. Some might find this behavior surprising, as having significantly more spreaders in a susceptible population should increase the peak of daily cases. From supplementary figures 1-5, we conclude that the model depends most sensitively on  $\beta$ ,  $a$ ,  $q_{max}$ ,  $t^*$ ,  $\epsilon$ , and  $\rho$ , since small variations cause



Supplementary Figure 4: **Effect of varying re-entry rate  $\rho$  on the total infected population and deaths.** (a) Total infected, and (b) deaths for  $\rho$  values ranging from 0-0.2. California fits were used for this comparison.

large changes in the shape of the daily total infected curve.



Supplementary Figure 5: **Effect of varying number of undetected infecteds  $U(0)$  on the total infected population and deaths.** (a) Total infected, and (b) deaths for  $U(0)/N$  values ranging from 0.1-100. California fits were used for this comparison.

## References

- [1] Johns Hopkins University. [https://github.com/CSSEGISandData/COVID-19/tree/master/csse\\_covid\\_19\\_data/csse\\_covid\\_19\\_time\\_series](https://github.com/CSSEGISandData/COVID-19/tree/master/csse_covid_19_data/csse_covid_19_time_series), 2020.
- [2] United States Census Bureau. <https://www2.census.gov/programs-surveys/popest/datasets/2010-2019/national/totals>, 2020.
- [3] The MathWorks, Inc. *Optimization Toolbox User's Guide: Least-Squares (Model Fitting) Algorithms*, r2017a edition, March 2017.
- [4] Pauline van den Driessche. Reproduction numbers of infectious disease models. *Infectious Disease Modelling*, 2(3):288–303, 2017.